Biophysical Chemistry 253 (2019) 106229

Contents lists available at ScienceDirect

Biophysical Chemistry

journal homepage: www.elsevier.com/locate/biophyschem

Research Article

Interdigitated lamellar phases in the frozen state: Spin-label CW- and FT-EPR

Erika Aloi[a], Rosa Bartucci[b,*]

[a] Department of Physics, Molecular Biophysics Laboratory, University of Calabria, 87036 Rende (CS), Italy
[b] Department of Chemistry and Chemical Technologies, University of Calabria, 87036 Rende (CS), Italy

HIGHLIGHTS

- DPPC/Lyso-PPC and DPPC/etOH interdigitated phases have been studied with spin-label CW- and FT-EPR.
- Librational motion occurs in the frozen interdigitated lipid dispersions.
- The mean-square angular amplitude of librations increases steeply for $T > 220$ K in any sample.
- In the interdigitated phases water exposure of the chain termini is comparable to that of the segments at the polar/apolar interface.

GRAPHICAL ABSTRACT

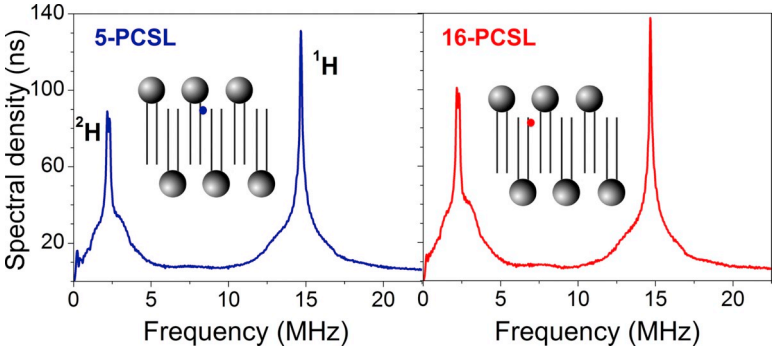

ABSTRACT

Interdigitated lamellar phases composed of dipalmitoylphosphatidylcholine (DPPC) and equimolar content of lyso-palmitoylphosphatidylcholine (Lyso-PPC) or DPPC hydrated in ethanol containing water (60% *v*/v) have been studied in the frozen state. Electron paramagnetic resonance spectra of labeled lipids at C5 or C16 carbon atom positions along the chain are indicative of segmental librational motion over the temperature range 120–260 K. For any dispersion, the mean-square-angular amplitudes of the librations are comparable for both label positions but are larger in DPPC/etOH than in DPPC/Lyso-PPC interdigitated sample. The temperature dependences of the librational amplitudes of the labels in the lipid matrices show a rapid increase at the dynamical transition at $T_d \approx 220$ K with an activation energy of 20–30 kJ/mol. Three-pulse electron spin echo envelope modulation by D_2O revealed comparable solvent accessibility and fractions of singly and doubly hydrogen-bonded nitroxides to deuterons for both positional isomers in the interdigitated lamellae at 77 K. The overall EPR results indicate that the interdigitated DPPC/etOH sample is more loosened packed compared to DPPC/Lyso-PPC sample. The findings of the present work obtained at cryogenic temperatures point out dynamic and molecular properties of interdigitated lamellae that contribute to the biophysical characterization of membrane model systems.

1. Introduction

Saturated, symmetrical-chain phosphatidylcholines (PCs) at full hydration in water self-assemble in bilayer lamellar phases, that are widely used as models of cell membranes [1]. Upon the temperature increase, the lipid bilayers undergo the thermotropic phase transitions between the ordered gel phases and from the gel to the fluid state. Specifically, bilayers of PCs undergo at T_p a low-energy pre-transition $L_{\beta'} \rightarrow P_{\beta'}$ between the $L_{\beta'}$ gel phase, in which the acyl chains are fully extended and tilted with respect to the bilayer normal, and the $P_{\beta'}$ gel phase, in which the bilayer is rippled; at T_m they undergo a high-energy and sharp main transition $P_{\beta'} \rightarrow L_\alpha$, associated with the melting of the lipid chains ([1,2] and references therein).

However, in the presence of an external inducer at a threshold

* Corresponding author.
E-mail address: rosa.bartucci@fis.unical.it (R. Bartucci).

https://doi.org/10.1016/j.bpc.2019.106229
Received 28 June 2019; Received in revised form 18 July 2019; Accepted 18 July 2019
Available online 21 July 2019

concentration, bilayers of PCs are converted to an interdigitated $L_{\beta i}$ phase in which the chain from opposing monolayers interpenetrate or interdigitate each other [3,4]. In this interdigitated lamellar phase, the terminal methyl groups of one monolayer are located near the interfacial region on the opposite side of the lipid lamellae. X-ray and neutron diffraction experiments have shown that chain interdigitation is found to occur in gel state lipids of dipalmitoylphosphatidylcholine (DPPC) lipids in the presence of various compounds such as glycerol and ethylene glycol [5], short-chain alcohols [6,7], chaotropic salts [8], micelle-forming lipids of lyso-palmitoylphosphatidilcholine (Lyso-PPC) [9], and resveratrol [10]. Structurally, these interdigitated gel phases are characterized by a reduction of the bilayer width, an increase in the area per polar head, and present chains fully extended and perpendicular to the plane of the bilayer. Calorimetrically, the pre-transition is abolished and the main transition involves a direct cooperative transformation $L_{\beta i} \rightarrow L_{\alpha}$ from the fully interdigitated gel phase to the conventional bilayer fluid phase upon increasing the temperature. Other experimental techniques, including Raman [11], fluorescence [12], spectrophotometry [13,14], spin-label EPR [10,14–20] have provided information on dynamics and molecular properties of the wide variety of samples with interdigitated chains. Most of these studies have been carried out in a temperature range that encompass the gel and the liquid-crystalline states of the samples, mostly in the range 283–323 K. Less investigated are the interdigitated lipid lamellae at low temperatures, in the frozen state.

Biophysical studies at low, cryogenic temperatures allow to highlight structural, dynamic and molecular features of biosystems that are inevitably present but not explicitly detectable at higher temperatures. Spin-label electron paramagnetic resonance (EPR) spectroscopy, both in continuous wave (CW-EPR) and in pulsed, Fourier Transform (FT-EPR) version, represents an efficient tool to investigate biosystems in the frozen state. By using CW-EPR and spin-echo methods of FT-EPR relevant properties have been addressed in spin-labeled biomembranes and proteins (see, i.e., [21,22]). These include the segmental librational dynamics, the direct accessibility of the solvent at specific region around the spin-label site, the transmembrane polarity profiles as revealed by polarity-sensitive spin-label EPR parameters, and the heterogeneity of protein substates. Spin-label EPR studies at low temperatures will therefore contribute to have a more complete biophysical characterization of interdigitated lipid assemblies.

In this work, we aim to investigate at cryogenic temperatures the interdigitated lamellar phases formed by DPPC and equimolar content of Lyso-PPC and DPPC in the presence of ethanol (etOH). By using chain labeled phosphatidylcholine at the beginning or at the terminal methyl end of the chain (5- and 16-PCSL, respectively) we focus on i) the segmental lipid librations in the frozen state over the temperature range 120–260 K by means of CW-EPR spectra and ii) the solvent (D_2O) accessibility in the proximity of the spin-label with electron spin echo envelope modulation spectroscopy (D_2O-ESEEM) at 77 K. The results are compared and discussed with previous ones obtained in bilayer lamellar phase of DPPC and interdigitated phase formed spontaneously by ether-linked dihexadecylphosphatidylcholine (DHPC) lipids [18,19].

2. Materials and methods

2.1. Materials

The synthetic lipids 1,2-dipalmitoyl-sn-glycero-3-phosphocholine (DPPC) and 1-palmitoyl-2-lyso-sn-glycero-3-phosphocholine (Lyso-PPC) were obtained from Sigma/Aldrich (St. Louis, MO). The spin-labeled lipids 1-palmitoyl-2-(n-(4,4-dimethyl-oxazolidine-N-oxyl) stearoyl)-*sn*-glycero-3-phosphocholine (*n*-PCSL with $n = 5$ and 16) were from Avanti Polar Lipids (Birmingham, AL). Ethanol and deuterium oxide (D_2O) (99.9 atom% ^2H) were also purchased from Sigma/Aldrich. All materials were used as purchased without further purification.

2.2. Sample preparation

The samples used were lipid dispersions prepared with the thin film hydration method. The sample DPPC/Lyso-PPC was prepared by dissolving in chloroform the required amounts of the lipids together with 0.5 mol% of the spin-labeled lipid *n*-PCSL. The solvent was first evaporated in a nitrogen gas stream and then under vacuum overnight. The dried lipid samples were fully hydrated with D_2O (final lipid concentration 50 mM), by heating and vortexing at 50 °C. The sample DPPC/etOH was prepared as described above except that the dried DPPC film was hydrated in ethanol containing D_2O (60% *v*/v). The hydrated lipid dispersions were concentrated at room temperature by centrifugation at 3000 rpm for 20 min in a bench-top centrifuge, the excess of water (D_2O) removed and the pellets transferred to standard (O.D. 4 mm) quartz EPR tubes for FT- and CW-EPR measurements.

2.3. EPR measurements

Conventional spin-label CW-EPR spectra were acquired between 120 and 260 K on a Bruker ESP-300 spectrometer operating at 9 GHz with 100-kHz field modulation, equipped with a Bruker ER 4201 TE_{102} rectangular cavity and a Bruker temperature controller.

Pulsed EPR data were collected at 77 K on an ELEXSYS E580 Fourier Transform (FT)-EPR spectrometer at 9 GHz (Bruker, Germany) equipped with a MD5 dielectric resonator and a CF 935P cryostat (Oxford Instruments, UK).

To obtain ESEEM spectra, three-pulse, stimulated echo ($\pi/2$-τ-$\pi/2$-T-$\pi/2$-τ-echo) decays were recorded by using microwave pulse widths of 12 ns, with the microwave power adjusted to give $\pi/2$-pulses. The time delay, T, between the second and the third pulses was incremented from 20 ns by 700 steps of 12 ns, whilst the inter-pulse separation, τ, between the first and second pulses was set equal to 168 ns to maximize the deuterium and proton modulations simultaneously. The magnetic field was set to the maximum of the EPR absorption. A four-step phase-cycling program was used to eliminate unwanted echoes.

For 3p-ESEEM experiments, samples were rapidly frozen in liquid nitrogen and then quickly accommodated into the pre-cooled cavity at 77 K.

Experiments were repeated to test data reproducibility.

3. Results and discussion

3.1. CW-EPR of 5- and 16-PCSL: segmental chain librations in interdigitated frozen dispersions

The CW-EPR spectra recorded at different temperatures between 120 and 260 K for 5- and 16-PCSL in interdigitated frozen samples of DPPC/Lyso-PPC and DPPC/etOH are shown in Fig. 1.

They are anisotropic powder spectra of spin-labeled lipids well incorporated and uniformly distributed in the host membrane matrix. In the low temperature regime (up to ca. 200–220 K) in any interdigitated sample the spectral anisotropy of both positional isomers is very large and of comparable extent, the resonance lines are inhomogenously broadened and the spectral width decreases only slightly with temperature. In the high temperature regime, the anisotropy reduces with temperature and the lines narrow progressively. Interestingly, by comparing the spectra in Fig. 1, the extent of anisotropy reduction with temperature is more evident at the chain termini and, in particular, in DPPC/etOH sample.

Quantitatively, the temperature variation of the spectral anisotropy can be evaluated by the plots of the motionally averaged hyperfine splitting, $2\langle A_{ZZ}\rangle$, measured between the two outer extreme of the spectra. In Fig. 2 are reported the dependences on temperature of $2\langle A_{ZZ}\rangle$ for 5- and 16-PCSL in the interdigitated samples.

The DPPC/Lyso-PPC interdigitated sample is characterized by a high value of the outer hyperfine splitting of about 6.90 mT common to

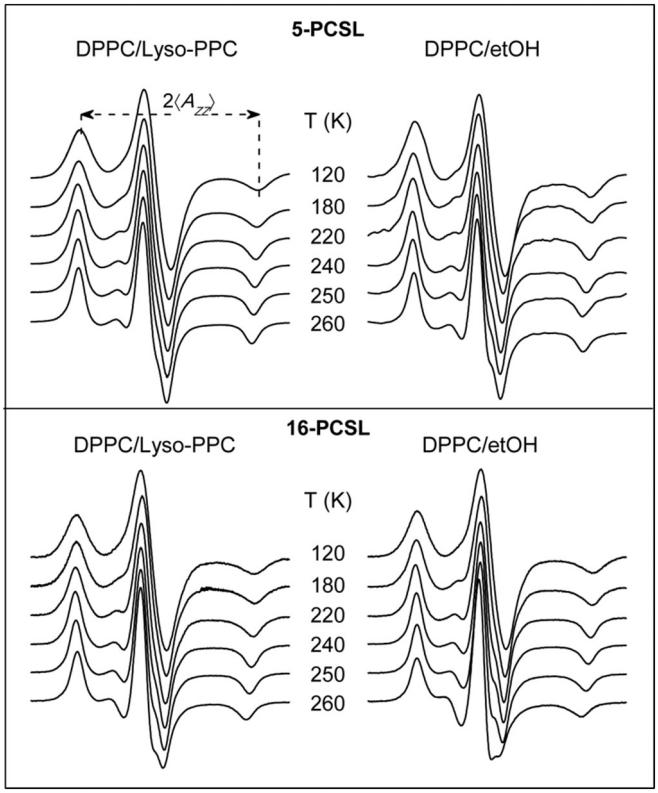

Fig. 1. CW-EPR spectra of 5- (upper panel) and 16-PCSL (lower panel) in interdigitated DPPC/Lyso-PPC and DPPC/etOH dispersions at different temperatures. Central field = 332.5 mT, sweep width = 10 mT.

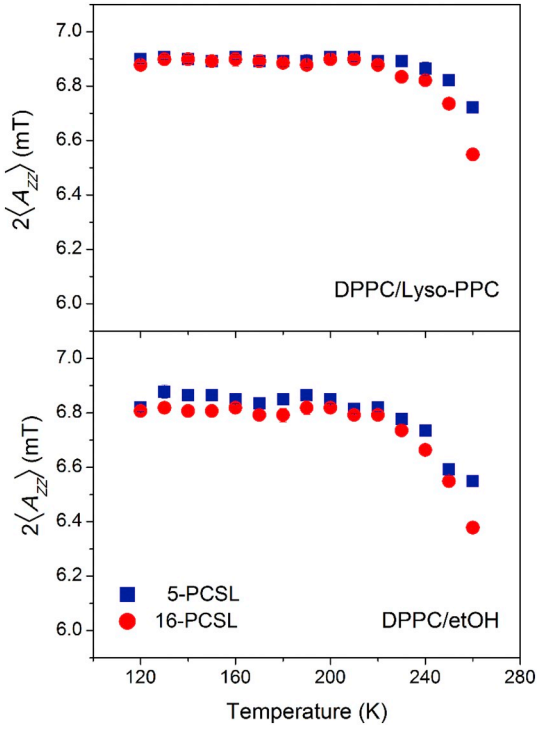

Fig. 2. Temperature dependence of 5- (squares) and 16-PCSL (circles) in DPPC/Lyso-PPC (upper panel) and DPPC/etOH (lower panel) interdigitated dispersions. Errors are smaller than the size of the symbols.

both spin-labels and independent on temperature up to 220 K. Then, the splitting reduces with temperature more rapidly for 16- than for 5-PCSL: $2\langle A_{ZZ}\rangle$ is 6.55 ± 0.02 mT for 16-PCSL and 6.72 ± 0.02 mT for 5-PCSL at 260 K. In the DPPC/etOH sample, the $2\langle A_{ZZ}\rangle$ values are slightly lower for 16- than for 5-PCSL and both slightly lower than those in DPPC/Lyso-PPC. Moreover, these values are temperature independent up to 200 K and then decrease more rapidly with respect to those in DPPC/Lyso-PPC reaching 6.38 ± 0.02 mT for 16-PCSL and 6.55 ± 0.02 mT for 5-PCSL at 260 K.

The finding that in both interdigitated samples the spectral anisotropy is comparable for the two extreme positions of chain labeling is an EPR signature of chain interdigitation. Indeed, in the molecular packing with interdigitated chains, an end-chain label such as 16-PCSL, located at the chain termini and normally probing the inner hydrocarbon region in a lipid bilayer, is restricted to an extent similar to that of a label much closer to the polar/apolar interface such as 5-PCSL, and both probe the same bilayer region of the opposing lamellae. The temperature variation of the spectral anisotropy of 5- and 16-PCSL, contrasts remarkably with that in bilayers of DPPC whose spectra of 5- are more anisotropic than those of 16-PCSL in the frozen [18] as well as in the gel state [16]. The lack of the bilayer midplane in the interdigitated phase, therefore, suppresses the limited chain-flexibility profile of increasing disorder and mobility on moving from the polar/apolar interface toward the terminal methyl end, which is detected in bilayers in the gel state by using cw-ESR of chain-labeled lipids [15,16].

An interesting feature of the results in Figs. 1 and 2 is that they indicate differences in the chain packing density between the two samples: the DPPC/etOH interdigitated lamellae are more loosened packed with respect to the DPPC/Lyso-PPC interdigitated sample. This can be seen in the lower spectral anisotropy and $2\langle A_{ZZ}\rangle$ values in the high-temperature regime of both positional isomers in DPPC/etOH dispersions. Differences in chain packing properties among various interdigitated samples were previously evidenced in the gel $L_{\beta i}$ phases. Indeed, the interdigitated state promoted in DPPC by glycerol is characterized by a uniformly tight packing of the interdigitated chains [11,16]. A loosened packing density was evidenced with 80 mg/ml etOH [15] or with chaotropic ions [8]. Other examples of loosened packed interdigitated bilayers are DHPC and 1,3 DPPC [15], that are known to spontaneously interdigitate in the gel phase.

Another remarkable aspect that emerges from the data in Figs. 1 and 2 is related to the segmental chain librational dynamics. The slight temperature variation of the spectral anisotropy in Fig. 1 and the temperature dependences characterized by constant $2\langle A_{ZZ}\rangle$-values in the low temperature regime and by a decrease for $T > 220$ K in Fig. 2 are typical of segmental chain librational motion [18,23,24]. This motion consists of rapid (in the T_2-timescale, nanosecond range) oscillations of small angular amplitude that occur simultaneously around the three perpendicular axes of the nitroxide spin-label group [24]. The motion manifests itself in the spin-label EPR spectra at low temperatures and cannot explicitly be visualized at the highest temperatures where it is hidden by the larger scale rotations. Evidence for librational motion has been obtained by linear and nonlinear CW-EPR spectroscopy in spin-labeled proteins [25–28] and by CW- and pulsed FT-EPR in spin-labeled frozen lipid dispersions, both conventional lipid bilayers and interdigitated lamellae [18,24,29]. Librational motion is also found to occur for spin-probe molecules in organic glasses [23,30].

The mean-square angular amplitude of librations can be evaluated from the motionally averaged hyperfine splitting according to the equation [23,31]:

$$\langle A_{ZZ}\rangle = A_{ZZ} - (A_{ZZ} - A_{XX})\cdot\langle\alpha^2\rangle \quad (1)$$

where $\langle A_{ZZ}\rangle$ is the halved experimental value of the hyperfine splitting, and A_{XX} and A_{ZZ} are the principal values of the hyperfine interaction tensor. The temperature dependences of $\langle\alpha^2\rangle$ for 5- and 16-PCSL in the interdigitated DPPC/Lyso-PPC and DPPC/etOH samples are shown in Fig. 3.

The plots in Fig. 3 inversely parallel those in Fig. 2 and from them can be pointed out that $\langle\alpha^2\rangle$ has a low value independent from temperature in the low temperature regime and then undergoes a rapid

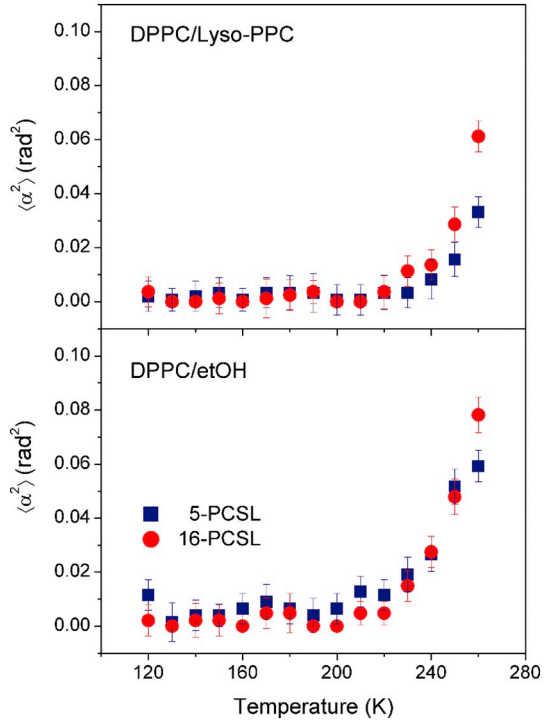

Fig. 3. Temperature dependence of the of 5- (squares) and 16-PCSL (circles) in DPPC/Lyso-PPC (upper panel) and DPPC/etOH (lower panel) interdigitated dispersions.

increase for $T > 220$ K for both samples. On going from 230 K to 240 K to 260 K, the angular amplitude for 5-PCSL (16-PCSL) increases from 3.3 ± 2.3° (6.0 ± 1.5°) to 5.2 ± 2.3° (6.7 ± 1.4°) to 10.4 ± 0.9° (14.1 ± 0.7°) in DPPC/Lyso-PPC and from 7.9 ± 1.3° (7.0 ± 1.3°) to 9.3 ± 1.1° (9.5 ± 1.0°) to 13.9 ± 0.7° (15.9 ± 0.7°) in DPPC/etOH, respectively. It is worthy to note that the angular amplitudes are higher in DPPC/etOH than in DPPC/Lyso-PPC. Again, this result is related to the difference in chain packing density between the two samples: the interdigitated lamellae are more loosened packed in the presence of ethanol and allow larger spin-label librational amplitudes.

It is of interest to compare the results obtained in the interdigitated DPPC/LysoPPC and DPPC/etOH samples with those for the ether-linked DHPC membranes, which spontaneously interdigitate in the gel state, and with those for the ester-linked DPPC, which form bilayers with noninterdigitated chains [18]. In the interdigitated DHPC sample, the $\langle\alpha^2\rangle$-values for both labels are very low and temperature independent up to 230 K and then increase steeply but with $\langle\alpha^2\rangle$ always greater at the chain termini than at the first segments over the entire temperature range. In the noninterdigitated DPPC sample, instead, the two positional isomers show a progressive increase in $\langle\alpha^2\rangle$ on increasing the temperature with $\langle\alpha^2\rangle$(16-PCSL) > $\langle\alpha^2\rangle$(5-PCSL) at any temperature [18].

The dependences on temperature of $\langle\alpha^2\rangle$ for 5- and 16-PCSL in the interdigitated samples shown in Fig. 3 are similar to those for chain-labeled lipids in DPPC with equimolar content of cholesterol [24], in bilayers of lipids extracted from native Na,K-ATPase membranes [32], for small spin-labels in glassy media [23,30], and for hydrated spin-labeled proteins [28,33]. More importantly, the temperature behavior of $\langle\alpha^2\rangle$ recorded by spin-label EPR is analogous to that of the mean-square displacement $\langle r^2\rangle$, measured in molecular glasses and various biosystems by neutron scattering or Mossbauer measurements [34–36]. In all cases, a rapid increase in amplitude of the atomic motion, or a marked change in the slope of its temperature dependence, is found at the dynamical transition temperature, T_d, of the systems around 200 K. From the data of the present study, a dynamical transition, associated

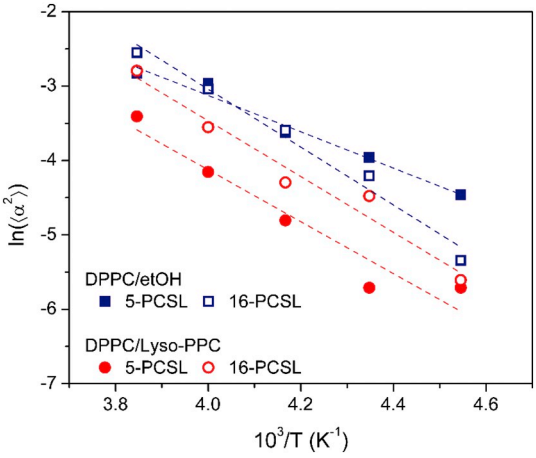

Fig. 4. Arrhenius plots characterizing the temperature dependence of the librational amplitude, ‹α²›, in the high-temperature regime for DPPC/Lyso-PPC (circles) or DPPC/etOH (squares) interdigitated samples spin-labeled with 5- (solid symbols) or 16-PCSL (open symbols). Dashed lines are linear regressions.

with the onset of stochastic librational motion, can be detected at $T_d \approx 220$ K in both interdigitated samples. This value is comparable to that reported for DHPC [18], whereas is higher than that reported in bilayers of saturated and unsaturated phospholipids in EPR experiments [18,29]. A dynamical transition in the range of 180–240 K has been identified in hydrated proteins and in natural membranes by using spin-label EPR [32,33], neutron scattering [36–39], Raman [40] and Mossbauer spectroscopy [41].

The progressive increase of $\langle\alpha^2\rangle$ for $T > T_d$ follows an Arrhenius law, which can be considered in the form $\langle\alpha^2\rangle \propto exp\left(\frac{E_a}{RT}\right)$ [35] . Thus, from the linear regressions of the Arrhenius plots in Fig. 4, the activation energy, E_a, for the onset of anharmonic motions can be evaluated. The obtained E_a values are 20.3 ± 1.8 kJ/mol for 5-PCSL and 32.4 ± 2.6 kJ/mol for 16-PCSL in DPPC/etOH; and 29.0 ± 4.6 kJ/mol for 5- and 31.2 ± 3.4 kJ/mol for 16-PCSL in DPPC/Lyso-PPC. These E_a-values are comparable to those reported previously with spin-label EPR in model membranes of various composition, such as DPPC bilayers with and without equimolar content of cholesterol and interdigitated DHPC lamellae, natural membranes and proteins [18,33,42]. Moreover, they are in the same range of those found in different biosystems with different scattering techniques [35,43].

3.2. D_2O-ESEEM of 5- and 16-PCSL: solvent accessibility in interdigitated frozen dispersions

Three-pulse (π/2-τ-π/2-T-π/2-τ-echo) D_2O-ESEEM measurements have been carried out to detect the solvent accessibility in the hydrocarbon region of the DPPC/etOH/D_2O sample with interdigitated chains [21]. In the left panel of Fig. 5 are reported the electron spin echo decays of the maximum amplitude of the stimulated echo vs. the interpulse spacing, T, at fixed τ = 168 ns at 77 K for 5- and 16-PCSL in the interdigitated DPPC/etOH lamellae.

The decay curves for both spin-labels show two modulations: superimposed to a slow oscillation with a period of about 0.4 μs, there is a rapid oscillation with a period of about 0.07 μs. The slow modulation is due to dipolar interactions of the spin-label with the ^{2}H-nuclear spin of the D_2O molecules, whereas the rapid modulation arises from interactions of the electron spin with nearby protons [44]. The modulation by D_2O is of interest because it comes specifically from the solvent.

Visualization and quantitation of the ^{2}H-modulation is better achieved after Fourier transformation, which yields the spectrum in the nuclear frequency domain. (For details on data processing, see [44,45]). Absolute-value frequency ESEEM spectra for 5- and 16-PCSL in DPPC/etOH (Fig. 5, right panel) show lines that are centered around

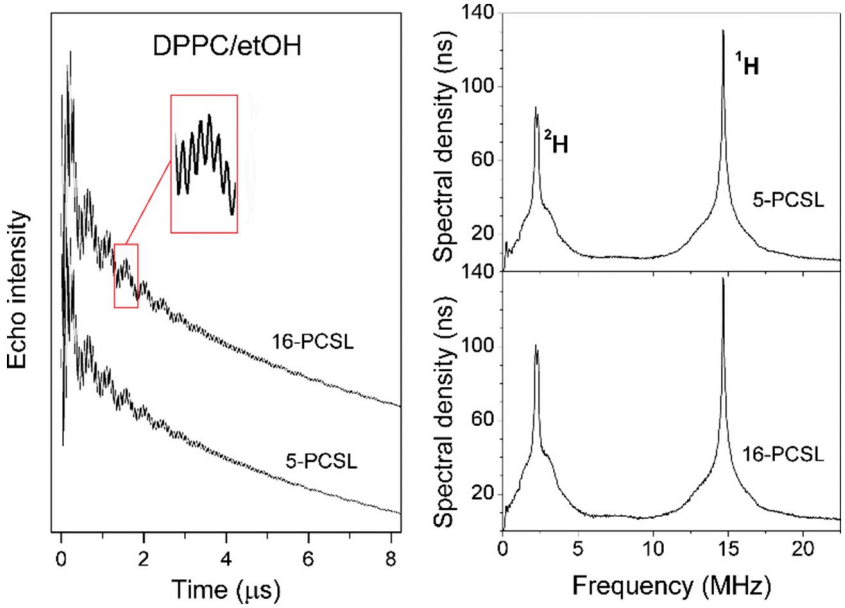

Fig. 5. (Left panel) Decay curves of the three-pulse electron spin echo amplitude with interpulse spacing, T, for 5-PCSL and 16-PCSL in DPPC/etOH hydrated in D_2O. (Right panel) Fourier Transform ESEEM spectra for samples as in the left panel. $T = 77$ K.

the deuterium ^{2}H-Larmor frequency at ca. 2.5 MHz and around the proton ^{1}H-Larmor frequency at ca. 15 MHz. The latter originates from matrix protons, whereas the former is specifically due to the solvent molecules. The deuterium ^{2}H-ESEEM signals consist of a sharp component superimposed to a broad component. The sharp component arises from free, not H-bonded D_2O molecules to the spin-label nitroxide -NO group, whereas the broad component is from H-bonded D_2O molecules to the nitroxide moiety [44]. The total amplitude of the deuterium ESEEM signal, I(^{2}H), is determined by the distance of the D_2O ^{2}H-nuclei from the spin-label and by the number of D_2O molecules neighboring the spin label within 0.5 nm [44]. This parameter, therefore, gives a direct measure of the extent of water (D_2O) penetration at the labeling site.

In the DPPC/etOH interdigitated phase, 5-PCSL, located at the first acyl chain segments, as well as 16-PCSL, located at the chain-ends, display an intense and comparable ^{2}H-signal, of ca. 89 ns and 101 ns, respectively. This is because in the molecular packing with interdigitated chains the inner apolar groups are transferred to solvent so that 5- and 16-PCSL probe almost the same lamellae environment at the polar/apolar interface. These results are in agreement with previous findings of the ^{2}H-ESEEM intensity dependence on the position of the spin-label, *n*-PCSL, along the chain in frozen interdigitated dispersions of DPPC/Lyso-PPC [20] and DHPC [19], which have shown that all the methylene segments are accessible to the solvent to a similar extent and are of elevated polarity. In particular, I(^{2}H) resulted to be ca. 90 ns (96 ns) in DPPC/Lyso-PPC and ca. 129 ns (144 ns) in DHPC for 5-PCSL (16-PCSL). Different is the positional dependence of I(^{2}H) in bilayers with noninterdigitated chains such as DPPC bilayers. Indeed, through cw- and pulsed EPR of chain-labeled lipids in DPPC bilayers, a sigmoidal transmembrane profile of polarity and solvent penetration is generally recorded in which the region close to the polar/apolar interface is of high polarity (high A_{ZZ} values) and accessible to the solvent (intense ^{2}H-signal, with I(^{2}H) for 5-PCSL ≈ 59 ns in DPPC and 121 ns in DPPC/cholesterol), whereas the innermost hydrocarbon region has reduced polarity (low A_{ZZ} values) and inaccessible to the solvent (^{2}H-signal absent) [42,44,46,47]. Thus, the loss of the bilayer midplane in the interdigitated phase abolishes the sigmoidal polarity and trans-hydrocarbon water accessibility profiles usually reported in lipid bilayers.

The analysis of the D_2O-signal of the frequency domain ESEEM spectra of spin-labels in lipid dispersions gives information on H-bond formation of the solvent molecules with the -NO nitroxide moiety [44]. Indeed, it is possible to evaluate the fraction of nitroxides that are singly, f_{1w}, and doubly, f_{2w}, bonded to D_2O molecules. This is done by considering the intensity of the broad component (that is due to spin-labels H-bonded to D_2O), the normalized ^{2}H-ESEEM intensity, I_0, for a nitroxide with a single hydrogen-bonded D_2O molecule (that is predicted by DFT calculations to be ≈115 ns), and by applying the mass-action law as described in [44].

A comparison of the fractions of 5 and 16-PCSL hydrogen bonded by one (f_{1w}) and two (f_{2w}) water molecules from ^{2}H-ESEEM spectra in a variety of interdigitated systems and in noninterdigitated bilayers of DPPC and DPPC/cholesterol 1:1 mol/mol are reported in Fig. 6.

From the data it can be seen that $f_{1w} > f_{2w}$ in any sample, suggesting that heterogeneity occurs in the structure of water surrounding the spin-labels incorporated in lamellar lipid assemblies. Moreover, by comparing the results for the interdigitated structures with those for DPPC bilayers, it is evident that for 5-PCSL the water penetration is higher in interdigitated lamellae than in bilayers due to the expansion

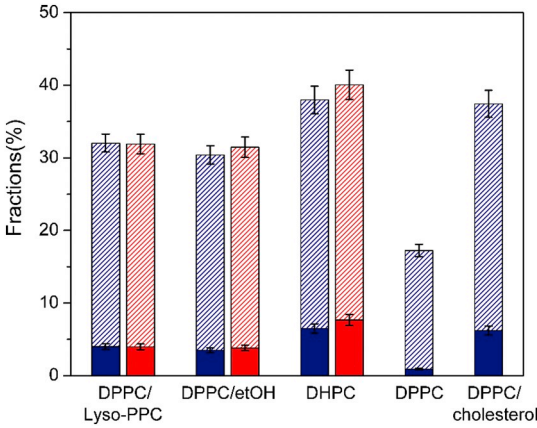

Fig. 6. Fractions of 5- (blue) and 16-PCSL (red) hydrogen bonded by one, f_{1w} (shaded), or two, f_{2w} (full), water molecules from D_2O-spectra of DPPC/Lyso-PPC, DPPC/etOH interdigitated samples and, for comparison, for DHPC interdigitated dispersions and DPPC and DPPC/cholesterol noninterdigitated bilayer dispersions. (For interpretation of the references to colour in this figure legend, the reader is referred to the web version of this article.)

in the area for polar head that drives the formation of the interdigitated phase. It is interesting to note that f_{1w} and f_{2w} in the interdigitated samples are comparable to those in bilayer membranes of DPPC/cholesterol, where the intervening cholesterol molecules space apart the polar heads allowing higher hydration at the interfacial region of the dispersions. In addition, the fractions (f_{1w} and f_{2w}) for spin-labels at the first position along the chain change in the order: f(DHPC) ≈ f(DPPC/cholesterol) > f(DPPC/Lyso-PPC) ≈ f(DPPC/etOH) > f(DPPC). This indicates that the interdigitated phase adopted spontaneously by DHPC lipids is the most hydrated and has properties similar to the polar region of bilayers of DPPC and equimolar cholesterol. A high level of hydration is also shown by the interdigitated phase induced in DPPC by Lyso-PPC or ethanol, whereas less hydrated is the polar/apolar interface in DPPC bilayers.

4. Conclusions

CW-EPR spectra and D_2O-ESEEM data of chain labeled lipids have been used to study frozen interdigitated lamellae induced in DPPC by ethanol or Lyso-PPC. The results obtained at low temperatures allowed us to expand on previous investigations and get deeper insight into molecular properties of interdigitated lipid assemblies that are usually investigated at higher temperatures through the gel state, up to the transition to the fluid state. New properties have been highlighted and discussed. They include the segmental chain librations, and the related dynamical transition and activation energies to cross low-energy barrier motion, and the accessibility of the solvent in the hydrocarbon zone as well as the hydrogen-bond formation between the spin-label groups and the D_2O molecules. Moreover, the study evidences that the two inducer molecules, ethanol and Lyso-PPC, confer different properties to the interdigitated phase: the chains result to be less densely packed and the angular amplitude of the librations is enhanced in the presence of ethanol than in the presence of the Lyso-lipid.

The results of the present work are of biophysical relevance because any molecule affecting the structure, the dynamics and the molecular properties of model membranes may influence specific membrane functions. In particular, surface-active molecules and lipids may also have an effect at the water-lipid interface in biomembranes, even though do not necessarily induce the chains to interdigitate.

Acknowledgments

The authors thank P. Foresta for helpful assistance during the experimental work.

References

[1] G. Cevc, D. Marsh, Phospholipid Bilayers. Physical Principles and Models, Wiley-Interscience, New York, 1987.
[2] D. Marsh, Handbook of Lipid Bilayers, 2nd ed., Taylor and Francis, New York, 2012.
[3] J.L. Slater, C.H. Huang, Interdigitated bilayer membranes, Prog. Lipid Res. 27 (1988) 325–359.
[4] E.A. Smith, P.K. Dea, Differential scanning calorimetry study of phospholipid membranes: the interdigitated gel phase, in: A.A. Elkordy (Ed.), Application of Calorimetry in a Wide Context – Differential Scanning Calorimetry, Isothermal Titration Calorimetry and Microcalorimetry, 2013 intechopen.com. 10.5772/2898.
[5] R.V. McDaniel, T.J. McIntosh, S.A. Simon, Nonelectrolyte substitution for water in phosphatidylcholine bilayers, Biochim. Biophys. Acta 731 (1983) 97–108.
[6] S.A. Simon, T.J. McIntosh, Interdigitated hydrocarbon chain packing causes the biphasic transition behavior in lipid/alcohol suspensions, Biochim. Biophys. Acta 773 (1984) 169–172.
[7] L. Lobbecke, G. Cevc, Effects of short-chain alcohols on the phase behavior and interdigitation of phosphatidylcholine bilayer membranes, Biochim. Biophys. Acta 1237 (1995) 59–69.
[8] B.A. Cunningham, L.J. Lis, Thiocyanate and bromide ions influence the bilayer structural parameters of phosphatidylcholine bilayers, Biochim. Biophys. Acta 861 (1986) 237–242.
[9] T.J. McIntosh, S. Advani, R.E. Burton, D.V. Zhelev, D. Needham, S.A. Simon, Experimental tests for protrusion and undulation pressures in phospholipids bilayers, Biochemistry 34 (1995) 8520–8532.
[10] E. Longo, F. Ciuchi, R. Guzzi, B. Rizzuti, R. Bartucci, Resveratrol induces chain interdigitation in DPPC cell membrane model systems, Colloids Surf. B 148 (2016) 615–621.
[11] T. O'Leary, I. Levin, Raman spectroscopic study of an interdigitated lipid bilayer dipalmitoylphosphatidylcholine dispersed in glycerol, Biochim. Biophys. Acta 776 (1984) 185–189.
[12] P. Nambi, E.S. Rowe, T.J. McIntosh, Studies of the ethanol-induced interdigitated gel phase in phosphatidylcholines using the fluorophore 1,6-diphenyl-1,3,5-hexatriene, Biochemistry 27 (1988) 9175–9182.
[13] E.S. Rowe, Induction of lateral phase separations in binary lipid mixtures by alcohol, Biochemistry 26 (1987) 46–51.
[14] R. Bartucci, S. Belsito, L. Sportelli, Neutral lipid bilayers interacting with chaotropic anions, Chem. Phys. Lipids 79 (1996) 171–180.
[15] J.M. Boggs, G. Rangaraj, A. Watts, Behavior of spin labels in a variety of interdigitated lipid bilayers, Biochim. Biophys. Acta 981 (1989) 243–253.
[16] R. Bartucci, T. Pali, D. Marsh, Lipid chain motion in an interdigitated gel phase: conventional and saturation transfer ESR of spin-labeled lipids in dipalmitoylphosphatidylcholine-glycerol dispersions, Biochemistry 32 (1993) 274–281.
[17] A. Stirpe, M. Pantusa, R. Guzzi, R. Bartucci, L. Sportelli, Chain interdigitation in DPPC bilayers induced by $HgCl_2$: evidences from continuous wave and pulsed EPR, Chem. Phys. Lipids 183 (2014) 176–183.
[18] E. Aloi, M. Oranges, R. Guzzi, R. Bartucci, Low-temperature dynamics of chain-labeled lipids in ester- and ether-linked phosphatydilcholine membranes, J. Phys. Chem. B 121 (2017) 9239–9246.
[19] M. Oranges, R. Guzzi, D. Marsh, R. Bartucci, Ether-linked lipids: spin-label EPR and spin echoes, Chem. Phys. Lipids 212 (2018) 130–137.
[20] E. Aloi, R. Bartucci, Solvent accessibility in interdigitated and micellar phases formed by DPPC/Lyso-PPC mixtures: D_2O-ESEEM of chain labeled lipids, Chem. Phys. Lipids 221 (2019) 39–45.
[21] R. Bartucci, D.A. Erilov, R. Guzzi, L. Sportelli, S.A. Dzuba, D. Marsh, Time-resolved electron spin resonance studies of spin-labelles lipids in membranes, Chem. Phys. Lipids 141 (2006) 142–157.
[22] R. Guzzi, R. Bartucci, Electron spin resonance of spin-labeled lipid assemblies and proteins, Arch. Biochem. Biophys 580 (2015) 102–111.
[23] S.A. Dzuba, Libration motion of guest spin probe molecules in organic glasses: CW EPR and electron spin echo study, Spectrochim. Acta A 56 (2000) 227–234.
[24] D.A. Erilov, R. Bartucci, R. Guzzi, D. Marsh, S.A. Dzuba, L. Sportelli, Librational motion of spin-labeled lipids in high-cholesterol containing membranes from echo-detected EPR spectra, Biophys. J. 87 (2004) 3873–3881.
[25] M.E. Johnson, Librational motion of an "immobilized" spin label: hemoglobin spin labeled by a maleimide derivative, Biochemistry 17 (1978) 1223–1238.
[26] J. Ruggiero, R. Sanches, M. Tabak, O.R. Nascimento, Motional properties of spin labels in proteins - effects of hydration, Can. J. Chem. 64 (1986) 366–372.
[27] H.J. Steinhoff, K. Lieutenant, J. Schlitter, Residual motion of hemoglobin-bound spin labels as a probe for protein dynamics, Z. Naturforsch. C Biosci. 44 (1989) 280–288.
[28] O.G. Poluektov, L.M. Utschig, S. Dalosto, M.C. Thurnauer, Probing local dynamics of the photosynthetic bacterial reaction center with a cysteine specific spin label, J. Phys. Chem. B 107 (2003) 6239–6244.
[29] N.V. Surovtsev, N.V. Ivanisenko, K.Y. Kirillov, S.A. Dzuba, Low-temperature dynamical and structural properties of saturated and monounsaturated phospholipid bilayers revealed by Raman and spin-label EPR spectroscopy, J. Phys. Chem. B 116 (2012) 8139–8144.
[30] S.V. Paschenko, Yu.V. Toropov, Temperature dependence of amplitudes of libration motion of guest spin-probe molecules in organic glasses, J. Chem. Phys. 110 (1999) 8150–8154.
[31] S.P. Van, G.B. Birrell, O.H. Griffith, Rapid anisotropic motion of spin labels. Models for motion averaging of the ESR parameters, J. Magn. Reson 15 (1974) 444–459.
[32] R. Guzzi, R. Bartucci, M. Esmann, D. Marsh, Lipid librations at the interface with the Na,K-ATPase, Biophys. J. 108 (2015) 2825–2832.
[33] D. Marsh, R. Bartucci, R. Guzzi, L. Sportelli, M. Esmann, Librational fluctuations in protein glasses, Biochim. Biophys. Acta, Proteins Proteomics 1834 (2013) 1591–1595.
[34] J. Fitter, R.E. Lechner, N.A. Dencher, Interactions of hydration water and biological membranes studied by neutron scattering, J. Phys. Chem. B 103 (1999) 8036–8050.
[35] P.W. Fenimore, H. Frauenfelder, B.H. McMahon, R.D. Young, Bulk-solvent and hydration-shell fluctuations, similar to alpha- and beta-fluctuations in glasses, control protein motions and functions, Proc. Natl. Acad. Sci. U. S. A. 101 (2004) 14408–14413.
[36] W. Doster, The protein-solvent glass transition, Biochim. Biophys. Acta, Proteins Proteomics 1804 (2010) 3–14.
[37] G. Schirò, C. Caronna, F. Natali, A. Cupane, Molecular origin and hydration dependence of protein anharmonicity: an elastic neutron scattering study, Phys. Chem. Chem. Phys. 12 (2010) 10215–10220.
[38] S. Magazù, F. Migliardo, A. Benedetto, B. Vertessy, Protein dynamics by neutron scattering: the protein dynamical transition and the fragile-to-strong dynamical crossover in hydrated lysozyme, Chem. Phys. 424 (2013) 26–31.
[39] J. Peters, J. Marion, F. Natali, E. Kats, D.J. Bicout, The dynamical transition of lipid multilamellar bilayers as a matter of cooperativity, J. Phys. Chem. B 121 (2017) 6860–6868.
[40] N.V. Surovtsev, E.S. Salnikov, V.K. Malinovsky, L.L. Sveshnikova, S.A. Dzuba, On the low-temperature onset of molecular flexibility in lipid bilayers seen by Raman scattering, J. Phys. Chem. B 112 (2008) 12361–12365.
[41] H. Frauenfelder, G. Chen, J. Berendzen, P.W. Fenimore, H. Jansson, B.H. McMahon, I.R. Stroe, J. Swenson, R.D. Young, A unified model of protein dynamics, Proc. Natl. Acad. Sci. U. S. A. 106 (2009) 5129–5134.
[42] R. Bartucci, R. Guzzi, D. Marsh, L. Sportelli, Chain dynamics in the low-temperature

phases of lipid membranes by electron spin-echo spectroscopy, J. Magn. Reson. 162 (2003) 371–379.
[43] J.R. Lewandowski, M.E. Halse, M. Blackledge, L. Emsley, Direct observation of hierarchical protein dynamics, Science 348 (2015) 578–581.
[44] D.A. Erilov, R. Bartucci, R. Guzzi, A.A. Shubin, A.G. Maryasov, D. Marsh, S.A. Dzuba, L. Sportelli, Water concentration profiles in membranes measured by ESEEM of spin-labeled lipids, J. Phys. Chem. B 109 (2005) 12003–12013.
[45] R. Bartucci, R. Guzzi, L. Sportelli, D. Marsh, Intramembrane water associated with TOAC spin-labeled alamethicin: electron spin-echo envelope modulation by D_2O, Biophys. J. 96 (2009) 997–1007.
[46] D. Marsh, Polarity and permeation profiles in lipid membranes, Proc. Natl. Ac. Sci. USA 98 (2001) 7777–7782.
[47] D. Marsh, Spin-label EPR for determining polarity and proticity in biomolecular assemblies: transmembrane profiles, Appl. Magn. Reson 37 (2010) 435–454.